

NATIONAL AIR INTELLIGENCE CENTER



MONTE-CARLO SIMULATION METHODS FOR FINITE FLAT PLATE WINDING FLOWS

by

Shi Yuzhong, Wu Qifen, Ren Bing



19950109 035

Approved for public release;
Distribution unlimited.

HUMAN TRANSLATION

NAIC-ID(RS)T-0919-92 15 November 1994

MICROFICHE NR: 94C00048/L

MONTE-CARLO SIMULATION METHODS FOR FINITE FLAT PLATE WINDING FLOWS

By: Shi Yuzhong, Wu Qifen, Ren Bing

English pages: 14

Source: Kongqidonglixue Xuebao, Vol. 9, Nr. 3, September
1991; pp. 324-329

Country of origin: China

Translated by: SCITRAN

F33657-84-D-0165

Quality Control: Ruth A. Peterson

Requester: NAIC/TATV/Paul F. Freisthler

Approved for public release; Distribution unlimited.

THIS TRANSLATION IS A RENDITION OF THE ORIGINAL FOREIGN TEXT WITHOUT ANY ANALYTICAL OR EDITORIAL COMMENT STATEMENTS OR THEORIES ADVOCATED OR IMPLIED ARE THOSE OF THE SOURCE AND DO NOT NECESSARILY REFLECT THE POSITION OR OPINION OF THE NATIONAL AIR INTELLIGENCE CENTER.

PREPARED BY:

TRANSLATION SERVICES
NATIONAL AIR INTELLIGENCE CENTER
WPAFB, OHIO

GRAPHICS DISCLAIMER

All figures, graphics, tables, equations, etc. merged into this translation were extracted from the best quality copy available.

STOP HERE

MONTE-CARLO SIMULATION METHODS FOR FINITE FLAT

PLATE WINDING FLOWS

/324*

Shi Yuzhong Wu Qifen Ren Bing

ABSTRACT

This article opts for the use of direct simulation Monte-Carlo methods to solve such problems as those associated with winding flows around flat plates of finite length. The methods in question are ones which go through tracking the movements of simulated molecules by computer in order to realize numerical value simulations. Collision calculations between simulated molecules are determined from statistical samplings. As far as collision models are concerned, respective selections were made for the use of hard sphere molecule models and inverse power law models. As far as simulation molecule and solid wall effects are concerned, option was made for the use of models which are made up from mixtures on the basis of ratios of fully diffused reflection and specular or mirror surface reflection. For the sake of the reliability of empirical test methods, calculations were also done of the one dimensional flow movements associated with such questions and Rayleigh problems and shock wave structures. Two dimensional calculations opted for the use of synchronous parallel programs. Numerical value results clearly showed that direct simulation Monte-Carlo methods were capable of relatively good simulations of a number of problems in rarefied gas mechanics. As far as two dimensional calculations are concerned, the machine time expended and the necessary content are both within ranges permitted by domestic machines.

SYMBOLS

L^*	Flat Plate Length	V_p	Most Probable Velocity in Undisturbed Gases
L	L^*/λ_∞ Nondimensional Flat Plate Length	V_r	Relative Velocity
m^*	Degenerate Mass	W_m	Nondimensional Collision Parameter Cut Off Value

* Numbers in margins indicate foreign pagination.
Commas in numbers indicate decimals.

M	Mach Number or the Oncoming Flow	ρ	Density
n	Simulation Molecule Number Density	λ	Average Free Travel
N_c	Simulation Molecule Number in Grid	ν	Inverse Power Law Index
p	Pressure	<u>Subscripts</u>	
t	Time	1	Value In Front of Wave
T	Temperature	2	Value Behind Wave
T_o	Overall Temperature of Oncoming Flow	f_r	Free Molecular Flow Full Diffusion Reflection Value
u	x direction speed	w	Wall Surface Value
v	y direction speed	∞	Oncoming Flow Value

INTRODUCTION

Normally, it is necessary to opt for the use of Boltzmann equation descriptions of the phenomena produced by rarefied gases. This equation is a nonlinear integral differential equation of distribution functions related to seven independent variables. Besides extremely particular special cases, equation analyses and solutions are extremely difficult. Moreover, as far as the application of finite differential methods of numerical value solutions is concerned, it is necessary to expend extremely large amounts of machine time as well as requiring extremely large internal storage. Because of this, it is not economical.

/325

Looking from the point of view of basic physical substance or quality, the microprocesses produced in rarefied gases are all random processes. At the end of the 1950's, people began to pay

attention to the similarity between this basic physical nature and Monte-Carlo simulation methods. Applying Monte-Carlo experimental particle methods to simulate rarefied gas dynamics problems, results were obtained. The first were Alder and Wainwright applying this method to study the process of gases tending toward equilibrium states in closed systems. After that, Bird and others made very great improvements and developments on Alder methods, setting up direct flow field simulation methods and successfully carrying out winding flow calculations for complex rotationally generated bodies [1] as well as techniques for the display of simple physical shape winding flows, relaxation processes, shock wave structures, shock wave reflection, and rarefied gas flow fields.

This article opts for the use of direct simulation Monte-Carlo methods to carry out numerical value solutions in finite length flat plate winding flow problems. For the sake of the accuracy of the testing methods, calculations were also done of such one dimensional questions as Rayleigh problems and shock wave structures. In conjunction with this, comparisons were made with reference results and theory.

I. SIMULATION TECHNIQUES

In flow fields, a control volume ADFC was selected (see Fig.1). It is assumed that, within a fixed time interval Δt_m , there are ΔN individual molecules which cross over the boundary surface AD and enter into the control volume. There are $\Delta N'$ individual molecules which cross over the boundary surface CF and leave the control volume. In the control volume, $N(t)$

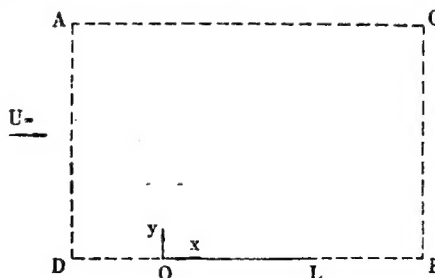


Fig.1 Control Volume

individual molecules move within it in conjunction with which collisions are given rise to. Monte-Carlo direct simulation techniques are to go through and carry out tracking calculations for these molecules and collisions between particles. Subsequent to this, statistical averaging obtains the relevant macro quantities. Due to machine internal storage and computer time limitations, it is not possible, nor is there any need, to directly track all actual molecules and carry out calculations in conjunction with that. During actual simulations, use is made of simulation molecules. Each simulation molecule represents many individual actual molecules. Due to this being the case, the number of molecules in the control volume is vastly reduced. However, there is a normal requirement for a number of simulated molecules in an individual grid which is not less than 20. In another regard, within the time interval Δt_m between going from t to $t + \Delta t_m$, simulation molecules aperiodically are all capable of meeting up with other simulation molecules or in collisions with solid walls and altering the mode of their movements. In order to realize simulation calculations, one assumes that simulation molecules, in this interval of time, do not give rise to any type of collision. Moreover, one takes the collisions which should take place in association with molecular systems in the time interval Δt_m and delays all of them to completion at the time instant $t + \Delta t_m$. In this way, when selecting the time interval Δt_m , it is necessary to satisfy the two limiting conditions of convection and collision below

$$U \Delta t_m / L_x \ll 1, V \Delta t_m / L_y \ll 1$$

Moreover, one must also satisfy

$$\Delta t_m \ll \tau_m$$

In these, U and V are, respectively, the average speed components associated with the x and y directions. L_x and L_y are,

respectively, the characteristic lengths associated with the x and y directions. τ_m is the average free time between two instances of collision between simulation molecules.

1. GRID DIVISIONS AND INITIAL FIELD DEFINITION

Statistical averaging and collision calculations all are carried out within each grid. Because this is the case, grid dimensions cannot be too large. Otherwise, the macro quantities obtained from statistical averaging would be unable to reflect macro physical configurations. In conjunction with that, it would cause a loss of reality for speeds from disturbances to propagation. In general, the required grid dimensions Δx and Δy are both not greater than the average free travel λ_m associated with molecules of the oncoming flow. This article, in calculations, has grid dimensions which, by contrast, are based on determinations associated with computer internal storage. Δx and Δy are selected as $0.5 \lambda_m$ or λ_m . In flat plate winding flow calculations, the y direction overall length is selected as $8 - 40 \lambda_m$. The x direction overall length is selected as $50 - 100 \lambda_m$.

/326

At a zero time instant, in each grid, the same number of simulation molecules are positioned. In each individual grid, the actual location of simulation molecules is determined on the basis of uniform distribution random sampling. The speeds which they possess are determined on the basis of equilibrium state speed distribution function sampling. In the same way, when implementing calculations, the number of simulation molecules in each grid must be determined on the basis of computer internal storage and the level of complexity of the problem. In carrying out shock wave structure problem calculations, at zero time instants, shock waves are positioned at the exact center of the control volume. The thickness is zero.

2. MOVEMENTS OF SIMULATION MOLECULES AND COLLISIONS BETWEEN SIMULATION MOLECULES

Within time interval Δt_m , the movements of each simulation molecule maintain uniform speed in a straight line

$$\begin{aligned}x(t + \Delta t_m) &= x(t) + u(t) \Delta t_m \\y(t + \Delta t_m) &= y(t) + v(t) \Delta t_m\end{aligned}$$

In the instant $t + \Delta t_m$, collision calculations are carried out within each grid. Within an individual grid, random sampling takes out two simulation molecules. On the basis of methods for acceptance or rejection, it is determined whether or not they give rise to collisions. If collision occurs, then, on the basis of the conservation of mass, the conservation of momentum, the conservation of energy, as well as the collision deviation angles given out by sampling, according to two dimensional collision theory, calculations give the speeds associated with the two simulation molecules after collision. Subsequent to this, calculations give "collision time" for the instance in question.

$$\Delta t = \frac{1}{N_c} \{ \pi W_m^2 (k/m^*)^{2/(r-1)} \cdot n V_r^{(r-6)/(r-1)} \}$$

Here, k is the molecular interaction law constant.

For each grid, one time measurement device was set up. As far as each instance of the occurrence of collisions is concerned, one then, on the corresponding time measurement device, adds on the instance of "collision time" in question. When the values of time measurement devices exceed $t + \Delta t_m$, within the time interval Δt_m , all calculations are completed for the collisions which should occur.

In the calculations of this article, in all cases, option is made for the use of hard sphere collision models and inverse power law collision models.

3. UPPER FLOW BOUNDARY TREATMENT

On the basis of numerical flux density, calculations are carried out of the number of molecules to enter the control volume within time interval Δt_m . Generally speaking, when actual molecular numbers are turned into simulation molecular numbers, the values obtained from calculations are not whole numbers. In the process of taking calculation values and turning them into integers or whole number values, the rounding off of fractional portions is determined by acceptance or rejection methods. Each individual simulation molecule's entry time into the control volume and its location for penetrating the boundary are determined from sampling. The speed of each simulation molecule is determined on the basis of sampling of average speeds for unidirectional equilibrium state distributions associated with U_∞ .

4. LOWER FLOW BOUNDARY CONDITION TREATMENT

Behind the lower flow boundary, as far as the placement of the image of a control volume simulation molecule system is concerned, all virtual molecule speeds and speeds of the original simulation molecules are the same. If, in the time interval Δt_m , the original molecules have escaped from the lower flow boundaries, then, the serial numbers are canceled. If, in the time interval Δt_m , there is a virtual or image molecule which enters the control volume, then, one takes that virtual or image molecule and sees it as a real simulation molecule and gives it a registration.

5. OTHER BOUNDARY TREATMENTS

Exterior boundary conditions are lens/mirror surface or specular reflection conditions. As far as the number of simulation electrons which escape from boundaries is concerned, adjustments are carried out on the basis of the law of the conservation of the total number of molecules within the entire control volume.

Solid wall conditions are made up on the basis of a mixture according to the ratio between the whole diffusion reflection and lens/mirror surface or specular reflection.

II. ANALYSIS OF RESULTS

/327

For Rayleigh problem calculation results see Fig.'s 2 - 4. These are, respectively, gas speed along the y direction, density, and temperature distributions. At the instant $t = 0$, flat plates use the speed U_0 to suddenly start up. At the instant $t = 4.43125 (\lambda_z / V_0)$, viscous diffusion has already reached a location approximately 6 average free travels from the surface of the plate. In the vicinity of the flat plate, gas flow speeds are small compared to flat plate speeds. Gas flow temperatures are high as compared to flat plate temperatures. This clearly shows that gas flows on plate surfaces show the appearance of speed slipping and temperature jumps. In the Fig.'s it is also shown that there is complete agreement with the results from Reference [1].

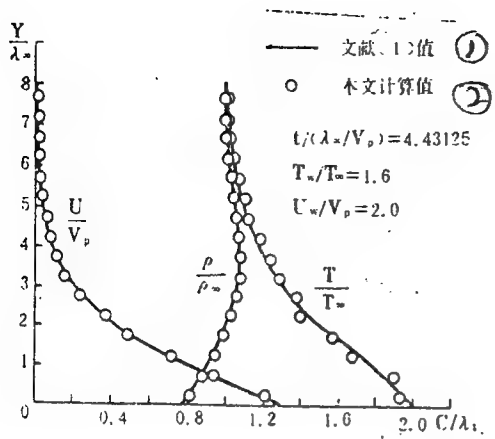


Fig.2 The Distribution for Tangential Velocity, Density, and Temperature

Key: (1) Reference [1] Values (2) Calculated Values from This Article

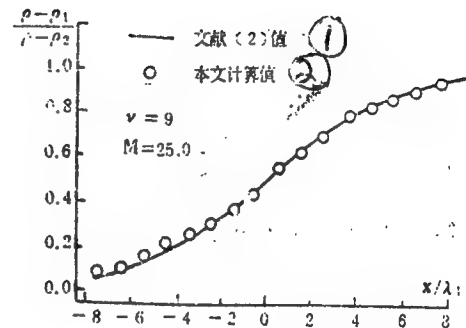


Fig.3 The Density Distribution

Key: (1) Reference [2] Values (2) Calculated Values from This Article

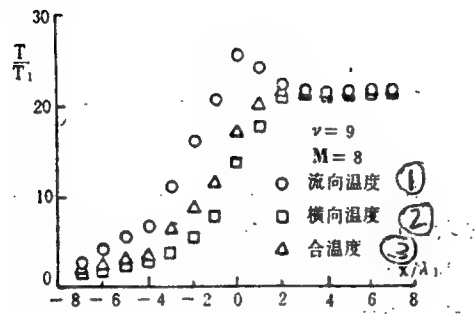


Fig.4 The Temperature Distribution

- (1) Flow Direction Temperature
- (2) Transverse Direction Temperature
- (3) Sum Temperature

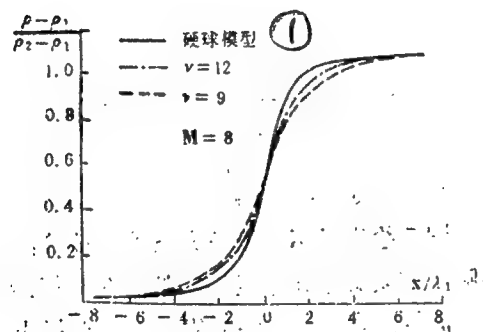


Fig.5 The Density Distribution

Key: (1) Hard Sphere Model

Calculation results for shock wave structure problems are given in Fig.5. In the Fig.'s, there are, respectively, given gas density distribution along the direction of flow as well as

flow direction and transverse direction temperature distributions. The calculated curves and the results from Reference [2] agree with each other. The asymmetrical natures of the calculated curves are given rise to due to the fact of relaxation processes during momentum and energy transfers. With regard to calculation results for different inverse power law indices ν , they clearly verified the formula for approximate calculations with regard to the influence of molecular models on shock wave thicknesses given in Reference [2]

$$L/\lambda_{\infty} \propto M_i^{(\nu-1)}$$

Here, L is the shock wave thickness. λ_{∞} is the average free travel in undisturbed gases. M_s (unclear) is the shock wave Mach number.

Winding flow calculation results for flat plates of finite length are shown in Fig.'s 6 - 8. Fig.6 gives wall surface pressure distributions. In conjunction with this, comparisons are carried out with experimental results from Becker [3]. This article opts for the use of simple single atom and molecule gas models to carry out numerical value simulations. There is mutual consistency with Becker's experiments with the inert gas Ar as medium. However, in order to show the influences of internally free molecules, in the same Fig., it gives experimental results taking N_2 as the medium. From the Fig., it is possible to see that calculations for 15% specular reflection agree relatively well with experimental results. It points out our properly selecting diffusion reflection and specular reflection /328 percentages. There is a great correlation with the degree of accuracy in the case of simulation analogs. On the rear edges of flat plates, due to this article's opting for the selection of flat plate finite length conditions, in making a comparison with the results of experiments, there is a relatively low pressure

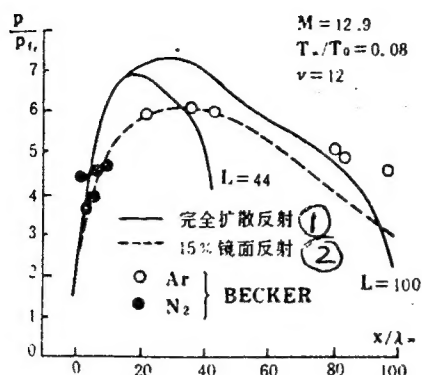


Fig.6 The Surface Pressure Distribution

Key: 1) Full Diffusion Reflection (2) 15% Specular Reflection

value. This point is also capable, from physics, of being explained. Due to the existence of flat plates, molecules close to the surface of the object gather together causing flat plate surface pressures to rise. This leads to experimental values being higher than calculated values. Reference [3] gives the experimental conditions to be, for Ar gas, $M_\infty = 12.66$, $T_w = 0.08 T_0$. This is consistent with this article's calculated conditions of $M_\infty = 12.9$, $T_w = 0.08 T_0$. For N_2 gas, $M_\infty = 11.18$, $T_w = 0.1 T_0$. There is some discrepancy here with the calculated conditions of this article.

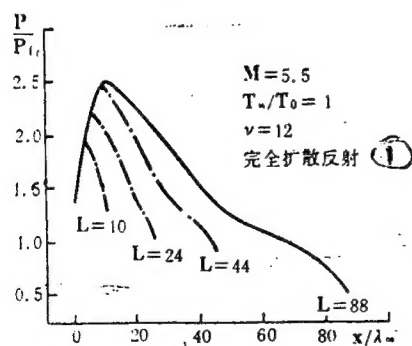


Fig.7 The Surface Pressure Distribution

Key: (1) Full Diffusion Reflection

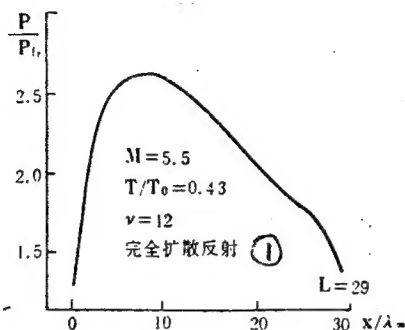


Fig.8 The Surface Pressure Distribution

Key: (1) Full Diffusion Reflection

Fig.7 gives a comparison of calculation results under conditions of different plate lengths L . From the calculation results, one can see the influence of plate length on wall surface pressures. This is primarily concentrated on the rear part of the plate. On the most forward portion of the plate, wall surface pressures receive no influence from plate length at all.

What is worth paying attention to is the fact that, besides trailing edges, the nondimensional pressure values for the whole plate are all greater than 1. This clearly shows that collisions between molecules as well as between molecules and wall surfaces cause wall surface pressures to rise.

REFERENCES

- [1] Bird, G. A., Oxford University Press (1976).
- [2] Bird, G. A., the Physics of Fluids, May (1973).
- [3] Becker, M., Rarefied Gas Dynamics, Suppl. 5, 1, edited by L. Trilling and H. Wachman, Academic Press, New York, (1969), 515—528.

DISTRIBUTION LIST

DISTRIBUTION DIRECT TO RECIPIENT

<u>ORGANIZATION</u>	<u>MICROFICHE</u>
B085 DIA/RTS-2FI	1
C509 BALLOC509 BALLISTIC RES LAB	1
C510 R&T LABS/AVEADCOM	1
C513 ARRADCOM	1
C535 AVRADCOM/TSARCOM	1
C539 TRASANA	1
Q592 FSTC	4
Q619 MSIC REDSTONE	1
Q008 NTIC	1
Q043 AFMIC-IS	1
E051 HQ USAF/INET	1
E404' AEDC/DOF	1
E408 AFWL	1
E410 AFDTC/IN	1
E429 SD/IND	1
P005 DOE/ISA/DDI	1
P050 CIA/OCR/ADD/SD	2
1051 AFTT/LDE	1
P090 NSA/CDB	1
2206 FSL	1

Microfiche Nbr: FTD94C000481L
NAIC-ID(RS)T-0919-92